ChemPubSoc Europe

DOI: 10.1002/chem.201400039

CHEMISTRY
A European Journal
Full Paper

Host–Guest Systems

Synthesis and Electronic Properties of 1,2-Hemisquarimines and Their Encapsulation in a Cucurbit[7]uril Host

Christian C. De Filippo,[a] Hao Tang,[b] Luca Ravotto,[c] Giacomo Bergamini,[c] Patrizio Salice,[a] Miriam Mba,[a] Paola Ceroni,*[c] Elena Galoppini,*[b] and Michele Maggini*[a]

Abstract: The synthesis of a new class of robust squaraine dyes, colloquially named 1,2-hemisquarimines (1,2-HSQiMs), through the microwave-assisted condensation of aniline derivatives with the 1,2-squaraine core is reported. In CH_3CN, 1,2-HSQiMs show a broad absorption band with a high extinction coefficient and a maximum at around $\lambda = 530$ nm, as well as an emission band centered at about $\lambda = 574$ nm, that are pH dependent. Protonation of the imine nitrogen causes a redshift of both absorption and emission maxima, with a concomitant increase in the lifetime of the emitting excited state. Encapsulation of the chromophore into a cucurbit[7]uril host revealed fluorescence enhancement and increased photostability in water. The redox characteristics of 1,2-HSQiMs indicate that charge injection into TiO_2 is possible; this opens up promising perspectives for their use as photosensitizers for solar energy conversion.

Introduction

Squaraines (SQs) **I** and **II** are organic chromophores that are derivatives of squaric acid. Among the most common SQ structures are the 1,3-regioisomers[1] (**I**) obtained by condensation of anhydrobases with squaric acid. These 1,3-SQ derivatives, which belong to the family of cyanine dyes, have been used as light harvesters or photosensitizers in organic[2] and hybrid organic–inorganic solar cells (DSCs)[3] or photodetectors[4] for their wide and highly tunable absorption range, as well as other favorable photophysical and electrochemical properties.

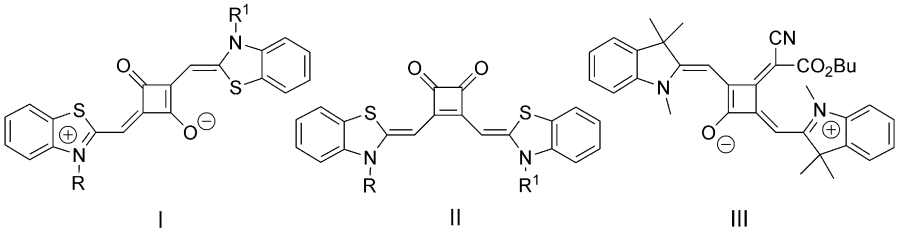

I II III

Specifically, 1,3-SQ dyes exhibit intense light absorption bands in the visible/near-infrared (NIR) region of the spectrum, NIR fluorescence with high quantum yields and nanosecond lifetimes,[4,5] and excited-state reduction potentials negative enough to allow electron transfer to acceptors such as fullerenes[6] or the TiO_2 conduction band.[7] In addition, the spectroscopic and redox properties of SQ dyes, in particular, the HOMO–LUMO levels, are tunable by varying the substituents on the squaric acid moiety.[8] 1,3-SQs also have a broad range of applications in different areas, such as imaging, nonlinear optics, and photodynamic therapy.[1] The 1,2-SQ regioisomers (**II**) have two cross-conjugated π-electron systems spanning from the heteroaromatic donor to the carbonyl acceptors and, for this reason, are regarded as merocyanine-type chromophores. 1,2-SQs can be prepared in excellent yields by condensing suitable precursors (i.e., the anhydrobase of the immonium salt **2**; Scheme 1) with squarate ester **3**.[9] The synthetic methods to access 1,2-SQs selectively, however, were developed only very recently and, to date, remain limited to a few reports.[9,10] For this reason, 1,2-SQs have not yet been studied as extensively as their 1,3-SQ counterparts, despite their attractive properties, including high electrochemical reversibility; increased solubility; absorption in the $\lambda = 550$ nm region, which is complementary to that of the 1,3-SQs; and low-lying HOMO levels, which are potentially useful to increase the open-circuit voltage (V_{OC}) of solar cells. Another class of compounds related structurally to 1,3-SQs are the core-substituted 1,3-SQs (**III**) that

[a] C. C. De Filippo, Dr. P. Salice, Dr. M. Mba, Prof. M. Maggini
Department of Chemical Sciences, University of Padova
Via Marzolo 1, 35131 Padova (Italy)
Fax: (+) 30 0498275050
E-mail: michele.maggini@unipd.it

[b] Dr. H. Tang, Prof. E. Galoppini
Department of Chemistry, Rutgers University
73 Warren Street, Newark, NJ - 07102 (USA)
E-mail: galoppin@rutgers.edu

[c] L. Ravotto, Dr. G. Bergamini, Prof. P. Ceroni
Department of Chemistry "G. Ciamician"
Via Selmi 2, 40126 Bologna (Italy)
E-mail: paola.ceroni@unibo.it

Supporting information for this article is available on the WWW under http://dx.doi.org/10.1002/chem.201400039.

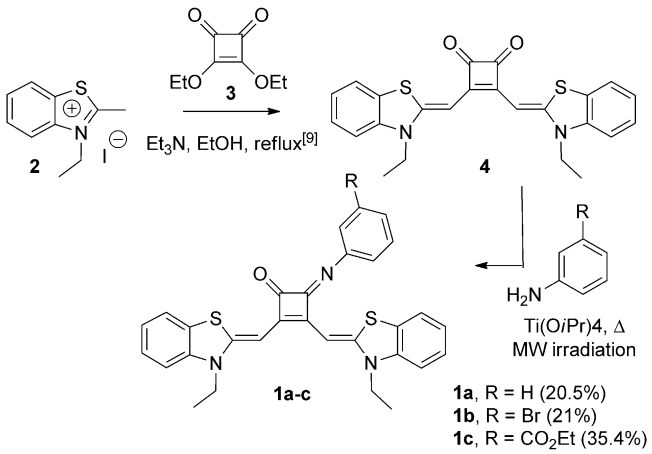

Scheme 1. Synthesis of 1,2-hemisquarimines **1a–c**.

have emerged as powerful panchromatic photosensitizers for DSCs.[11]

Herein, we report a further development of 1,2-SQ chemistry, namely, the synthesis of compounds **1a–c** through the condensation of **4** with the corresponding aniline derivative in the presence of titanium(IV) isopropoxide under MW irradiation (Scheme 1). We have named these new condensation products hemisquarimines (HSQiMs). The phenylimine functional group can bear different substituents, including a bromine atom for further functionalization through cross-coupling chemistry or an alkyl ester group that, upon hydrolysis, can anchor to TiO_2. More importantly, the conjugated 1,2-HSQiM structure allows, at least in principle, the directionality of electron flow, in the carboxylic push–pull photosensitizer, from the electron-rich benzothiazole moiety toward the semiconductor surface to be maintained. This is a fundamental molecular design prerequisite for electronic coupling between the LUMO of the sensitizer and the oxide conduction band in DSCs. Furthermore, herein, the photophysical and electrochemical properties of 1,2-HSQiMs **1a–c**, are presented, along with a study of the host–guest complex of **1a** with cucurbit[7]uril (CB[7]). The molecular structures and relative dimensions of CB[7] and **1a** are shown in Figure 1. SQs, similar to numerous other organic dyes, have the tendency to aggregate and, in some cases, they may also photodegrade. This behavior is particularly observed on nanostructured semiconducting surfaces such as TiO_2, upon

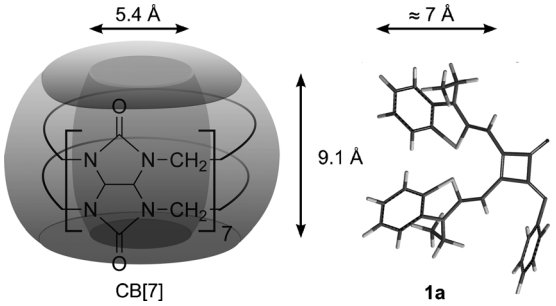

Figure 1. Molecular structure and dimensions of CB[7] and **1a**.

which photostability and decreased aggregation are important for applications involving charge transfer. The use of molecular hosts to encapsulate dyes, in solution and on semiconductor surfaces, is a strategy that is increasingly employed to overcome such problems, as well as to enhance emission properties, influence charge transfer, and, generally, to shield the chromophore and achieve binding control.[12]

CB[7], which is a water-soluble macrocyclic host composed of seven glycoluryl units and methylene units, is part of the broader cucurbit[*n*]uril family (CB[*n*], typically $n=5$–8 and 10).[13] CB[*n*] hosts, especially CB[7], offer significant advantages over other host molecules, such as crown ethers or cyclodextrins, because CB[*n*] can bind to molecular guests with high binding affinities.[14] For example, the binding affinities of adamantane derivatives ($>10^{12}\,M^{-1}$)[14b] to CB[7] are at least 10^7 times higher than that to β-cyclodextrin (10^4–$10^5\,M^{-1}$).[15] The dominant driving forces for CB[*n*]–guest binding are hydrophobic effects and ion–dipole interactions between the carbonyl-lined portals of CB[*n*] and the guest cation that lead to a slow dissociation process of the guest in CB[*n*] cavities.[16] In particular, binding to CB[7] stabilizes dyes against photobleaching,[17] reduces dye aggregation,[18] enhances the dye fluorescence emission,[19] and may lead to electrochromic effects.[20]

Results and Discussion

Synthesis

The synthesis of 1,2-HSQiMs **1a–c** is shown in Scheme 1. It was achieved in one step by the condensation of **4**[9] with the specific aniline, in the presence of $Ti(OiPr)_4$ under microwave (MW) irradiation to overcome the high stability of the 1,2-diketone system against nucleophilic attack. The investigation of the effect of MW irradiation indicates that the best conversions can be obtained within the temperature range of 80–90 °C for 2.5–8 min of reaction time. Under these conditions, the product imines **1a–c** were isolated in 21–35% yield after chromatographic purification, which turned out to be a rather difficult task because highly polar **1a–c** tended to irreversibly bind onto the stationary phase (either silica gel or alumina) of the chromatographic column. The rest was mostly unreacted **4** and a complex mixture of compounds. In the case in which aniline was used, TLC over neutral alumina, with toluene/AcOEt (8:2) with 3% MeOH as the eluent, showed the presence of nonfluorescent side products with a retention factor (R_f) of >0.8. Fluorescent 1,2-HSQiM **1a** appeared at $R_f=0.64$, as confirmed by ^1H and ^{13}C NMR spectroscopy and MS analyses of the isolated product. The nonsymmetrical 1,2-SQ core of **1a–c** is evidenced in the ^1H NMR spectrum by two resonances for the alkenyl protons between $\delta=5.5$ and 6 ppm (see the Supporting Information). TLC analysis of the crude mixture showed traces of fluorescent 1,2-SQiM ($R_f=0.73$) in which both carbonyl groups of **4** were condensed with aniline, as observed by MS analysis of an isolated fraction. Unreacted **4** was detected as a fluorescent spot at $R_f=0.16$. Decomposition of the starting 1,2-SQ substrate and products was observed at temperatures of >90 °C and prolonged MW irradiation. Although

not fully compatible with **4** and product imines, the use of highly oxophilic Ti^{IV} species and MW heating proved suitable to give the expected product imines **1a–c** in moderate yields. Further conditions are currently being investigated, in particular, the use of alternative Lewis acid activation, to increase the conversions and minimize the formation of side products. IR and Raman vibrational spectroscopies were used to characterize the donor–acceptor nature of both derivatives **4** and **1a**. As mentioned earlier, the structure of **4** contains a cross-conjugated π-electron system that links four end groups: two donor-linked (benzothiazole) units (D) and two carbonyls with electron-accepting characteristics (A). In analogy with other merocyanine systems,[21] a few vibrational modes are simultaneously active in both the IR and Raman spectra at $\tilde{\nu}=1590$, 1500, 1420, and 1160 cm^{-1}, (Figure S1 in the Supporting Information); this indicates that the D–A groups in **4** are strongly coupled. Derivative **1a**, in which one of the cyclobutenyl carbonyl groups has been replaced by a phenylimine group, shows IR and Raman spectra similar to those recorded for **4**, except for the signal corresponding to the acceptor units, which is now split into two components for the carbonyl and imine groups at $\tilde{\nu}=1490$ and 1520 cm^{-1}, respectively (Figure S1 in the Supporting Information). This also suggests that in **1a** the D–A groups are strongly coupled, which is in agreement with the large dipole moment calculated by DFT.

Theoretical calculations

DFT calculations carried out for **4** and **1a** suggest that a *syn* conformation is favored for both. In the case of **4**, this finding is in accordance with diffraction analysis data.[9] Also, both molecules have a large dipole moment (about 10 D). The formation of the imine leads to decreased delocalization of the frontier orbitals onto the heterocyclic ring and a small increase in the HOMO–LUMO gap compared with that of **4** (Figure 2).

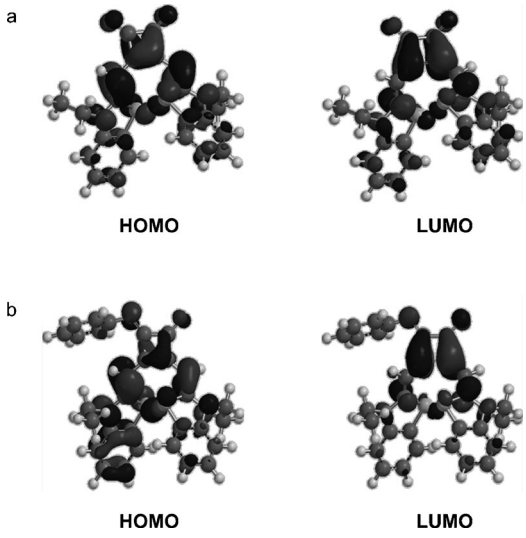

Figure 2. Contour plots for the HOMO and LUMO orbitals of **4** (a) and **1a** (b).

Photophysical properties in acetonitrile

The absorption spectra of compounds **1a–c** in CH_3CN exhibit an almost identical shape with a band maximum at $\lambda \approx 530$ nm (Table 1). Interestingly, all spectra present a high molar absorption coefficient over a wide wavelength range, spanning from the UV to about $\lambda = 600$ nm. Figure 3 reports the absorption characteristics of derivative **1a**, which can be considered a representative example of a 1,2-HSQiM. A modest solvatochromism is observed: for example, the absorption band maximum of **1a** shifts from $\lambda = 527$ to 534 nm upon going from CH_3CN to DMF.

Table 1. Photophysical properties of the investigated compounds and their protonated forms in air-equilibrated CH_3CN at room temperature.

	λ_{abs} [nm]	$\varepsilon_{max}/10^4$ [$cm^{-1}\,M^{-1}$]	λ_{em} [nm]	Φ_{em}	τ [ns]
1a	527	5.0	574	1.4×10^{-3}	<0.1
1a·H^+	466	3.3	635	2.1×10^{-2}	0.4
	556	3.6			
1b	531	6.3	572	1.7×10^{-3}	<0.1
1b·H^+	466	4.5	640	1.4×10^{-2}	0.4
	551	3.9			
1c	529	6.2	572	2.1×10^{-3}	<0.1
1c·H^+	467	4.2	639	1.7×10^{-2}	0.4
	552	4.0			
4	519	11.1	542	7.2×10^{-3}	<0.1

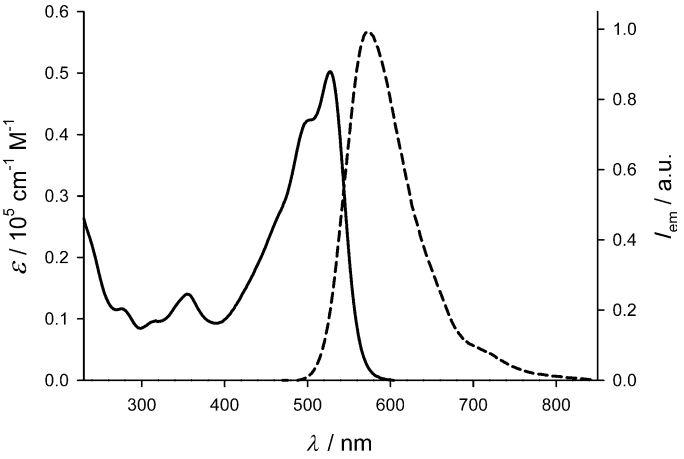

Figure 3. Absorption (——) and emission (-----) spectra of **1a** in CH_3CN.

No change in the absorption spectral shape was observed within the concentration range 10^{-6}–10^{-4} M explored; thus suggesting no aggregation phenomena. Figure 3 also shows the emission spectrum of compound **1a** (dashed line) in CH_3CN at room temperature, with a band maximum at $\lambda = 574$ nm: no significant difference in the band maximum was observed for 1,2-HSQiMs **1a–c** (Table 1). The emission quantum yields (Φ_{em}; Table 1) are quite low, with a slight increase upon going from compound **1a** to functionalized derivatives **1b** and **1c**. The fluorescence lifetimes are very short and below the instrumental resolution ($\tau < 100$ ps). Compounds **1a–c** exhibit

photophysical properties very similar to compound **4**, apart from a broader and less intense lowest energy absorption band. All of the investigated compounds show a very high photostability upon irradiation at $\lambda = 436$ nm in CH_3CN ($\Phi_{photoreact} < 1 \times 10^{-4}$). This result is encouraging in view of potential applications of 1,2-HSQiMs in solar energy conversion devices.

Acid–base behavior in acetonitrile

The absorption spectra of compound **1a** upon titration with CF_3SO_3H in CH_3CN (Figure 4a) show a progressive decrease of the most intense peak at $\lambda = 527$ nm, with a simultaneous growth of two bands with maxima at $\lambda = 466$ and 556 nm, respectively.

The presence of several isosbestic points suggests the direct transformation of one species into another, which is compatible with a single protonation step. Analysis of the spectral changes with the SPECFIT software, upon acid addition to **1a**, gave a pK_a value of 6.3. Because no spectral changes were observed for compound **4**, under the same experimental conditions as those used for the characterization of **1a**, it is reasonable to assume that protonation occurs at the imine nitrogen. Fluorescence spectra, recorded upon excitation at an isosbestic point ($\lambda_{exc} = 367$ nm), show the progressive decrease of the $\lambda =$ 574 nm band with the growth of a 5-fold more intense emission, with a maximum centered at $\lambda = 635$ nm (Figure 4b). The same behavior was observed for all investigated compounds, with a different degree of increase of the quantum yield depending on the specific substituents in the phenyl ring of the imine function (Table 1). The lifetimes of the emitting excited state show a concomitant increase to 0.4 ns. The observed spectral changes are completely reversible upon addition of tributylamine.

Electrochemical characterization in acetonitrile

Cyclic voltammograms of compound **1a** (Figure 5), recorded in CH_3CN (0.1 M tetraethylammonium hexafluorophosphate

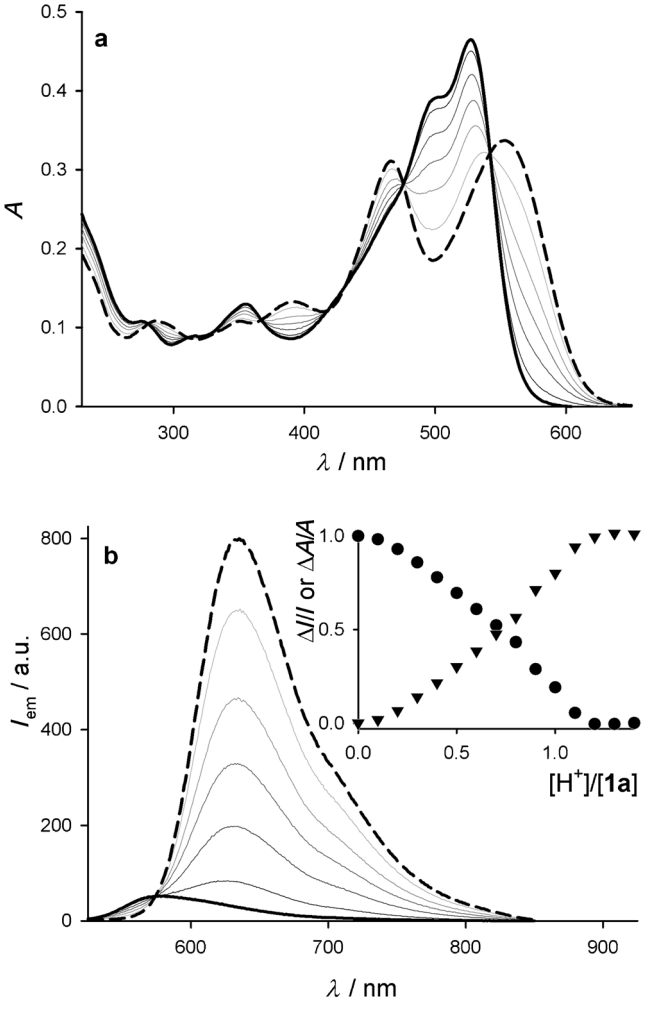

Figure 4. Absorption (a) and emission (b) spectra of compound **1a** ($c = 9.2 \times 10^{-6}$ M) upon titration with CF_3SO_3H in CH_3CN: from 0 (——) to 1.4 equiv (-----) of acid; $\lambda_{ex} = 367$ nm. Inset: the normalized changes of absorbance at $\lambda = 500$ nm (circles) and emission intensity at $\lambda = 670$ nm (triangles) with respect to the added equivalents of acid.

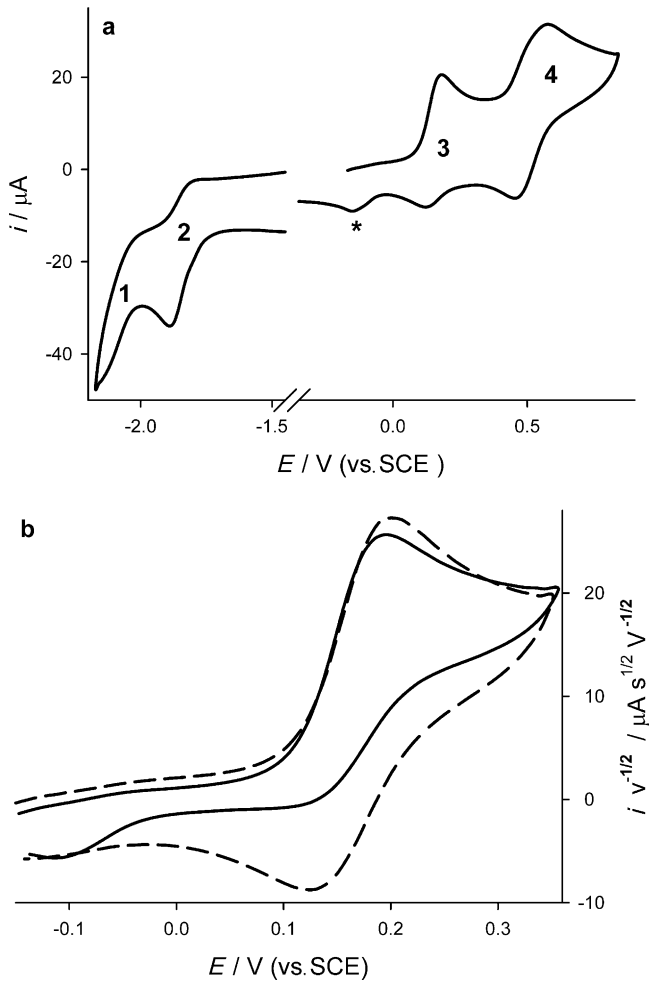

Figure 5. Cyclic voltammetry (CV) results for compound **1a** in $CH_3CN/TEAPF_6$ at room temperature: scan rate $V = 0.5$ (a), 0.1 (b, ——), and 1 $V s^{-1}$ (b, -----). For comparison purposes, cyclic voltammograms in b) report the value of $I/V^{1/2}$.

($TEAPF_6$)) at room temperature, show two one-electron-transfer processes both in the cathodic (peaks 1 and 2 in Figure 5a) and anodic region (peaks 3 and 4 in Figure 5a).

Processes 1, 2, and 4 are chemically and electrochemically reversible, whereas process 3 is associated with a chemical reaction, the product of which is re-reduced (corresponding to the peak marked with * in Figure 5a). Complete chemical reversibility is attained at scan rates higher than $1\,V\,s^{-1}$, as reported in Figure 5b. Compound **4** shows a very similar value of the reduction potential for the first process in the cathodic region (Table 2). The oxidation processes are shifted to less

Table 2. Oxidation (ox.) and reduction (red.) potentials ($E_{1/2}$ in V vs. a standard calomel electrode (SCE)) of compounds **1a** and **4** in CH_3CN at room temperature (0.1 M $TEAPF_6$).

Compound	Ox.	Red.
1a	+0.52	−1.82
	+0.16	−2.07
4	+0.75	−1.80
	+0.28	

positive potentials and the first process is again associated with a chemical reaction, and attains reversibility at high scan rates. The electrochemical HOMO–LUMO gap (≈2.0 eV) is in good agreement with the spectroscopic energy gap ($E_{0\text{-}0}$ ≈2.2 eV, as estimated from the emission maximum reported in Table 1). From the spectroscopic energy ($E_{0\text{-}0}$) and the ground-state redox potential for the oxidation process (E_{ox}), we can estimate the redox potential for the excited state (E^*_{ox}) by the approximated formula: $E^*_{ox} = E_{ox} - E_{0\text{-}0}$. In the case of **1a**, $E^*_{ox} = -1.82$ V versus SCE is substantially higher than the conduction band of TiO_2, which allows activationless charge injection into TiO_2.

Properties of 1a in aqueous solutions and encapsulation in CB[7]

The absorption and emission properties of **1a** were studied in aqueous solutions and at different pH values, in a solvent and under conditions relevant to encapsulation in CB[7]. The absorption and emission spectra of **1a** were strongly pH dependent (Figure S2 in the Supporting Information). The fluorescence spectrum for **1a** at pH 5.7 was very weak and increased about 4-fold when the pH was decreased to 1.1, as shown in the inset of Figure S2 in the Supporting Information. The complexation of **1a** in CB[7] was studied in deionized water (pH 6.9) and under acidic solutions, in which the non-protonated (**1a**@CB[7]) and protonated (**1aH**$^+$@CB[7]) forms of the complex were predominant, respectively. The shape of the absorption spectrum for **1a** in deionized water changed dramatically upon the addition of CB[7]: the band maximum shifts from $\lambda = 474$ to 556 nm (Figure 6), which indicates the formation of the **1a**@CB[7] complex. The absorption spectrum of **1a**@CB[7] was comparable to that of **1a** in CH_3CN (curve c in Figure 6), suggesting that the hydrophobic microenvironment

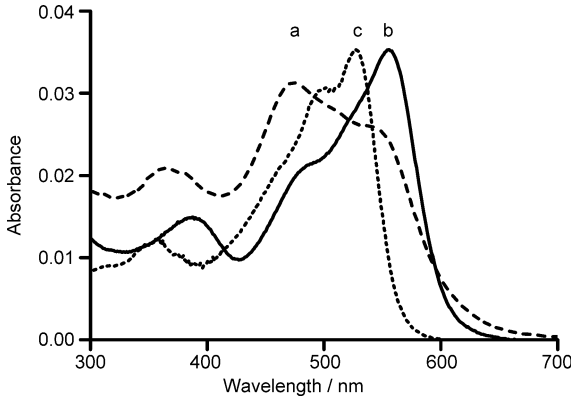

Figure 6. Absorption spectra for aqueous solutions of **1a** in the absence (a; $\lambda_{max} = 474$ nm) and in the presence (b; $\lambda_{max} = 556$ nm) of 250 μM CB[7]. pH 6.9. c) The absorption spectrum for **1a** in CH_3CN.

provided by the cavity of CB[7] for **1a** was similar to that provided by organic solvents.[21] The isotherm for **1a** binding to CB[7] was determined by adding stock solutions of CB[7] to a solution of **1a** (Figure 7). The data fit well with a 1:1 CB[7]/**1a** binding model and the equilibrium binding constant for CB[7]–**1a** complex was determined as $(4.18 \pm 0.09) \times 10^4\,M^{-1}$, according to three independent experiments.

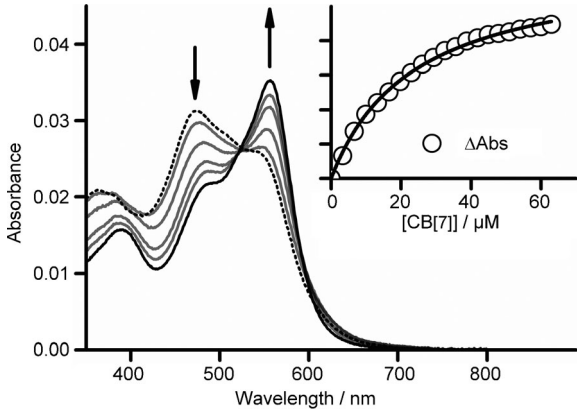

Figure 7. Binding isotherm for **1a** (2.5 μM) binding to CB[7] (0–63 μM) in deionized water (pH 6.9). Following the arrow: [CB[7]] = 0 (•••••), 3.34, 9.97, 23.0, 32.5, and 62.9 μM (——). Inset: Absorbance change of **1a** at $\lambda = 556$ nm with the addition of CB[7]. The curve represents the fit of data to the model of 1:1 CB[7]/**1a** binding with a value of $(4.18 \pm 0.09) \times 10^4\,M^{-1}$ recovered for the equilibrium binding constant (K).

The formation of **1a**@CB[7] in deionized water was probed by steady-state fluorescence (Figure S3 in the Supporting Information). The addition of CB[7] to an aqueous solution of **1a** led to a 21-fold enhancement of fluorescence intensity, and a redshift of fluorescence emission maximum from $\lambda = 488$ to 621 nm (inset to Figure S3 in the Supporting Information). The shape of the absorption spectrum of **1a** in water at pH 1.6 changed with the addition of CB[7], although large shifts were not observed (Figure S4 in the Supporting Information). The broadening of the spectrum of **1a**, compared with that ob-

served in the presence of CB[7], is ascribed to the coexistence of **1a** and **1aH**$^+$. The formation of the **1aH**$^+$@CB[7] complex at pH 1.6 was confirmed by the 4.5-fold enhancement and sharpening of the spectral bands upon CB[7] addition in the steady-state fluorescence spectra (Figure S5 in the Supporting Information).

A series of absorption spectra were recorded for the aqueous solution of **1a**@CB[7] upon addition of HCl to check whether **1aH**$^+$@CB[7] could be formed (Figure 8). The decrease in the absorption peak at $\lambda = 556$ nm and the increase in the peak at $\lambda = 432$ nm upon addition of HCl indicated the formation of **1aH**$^+$@CB[7].

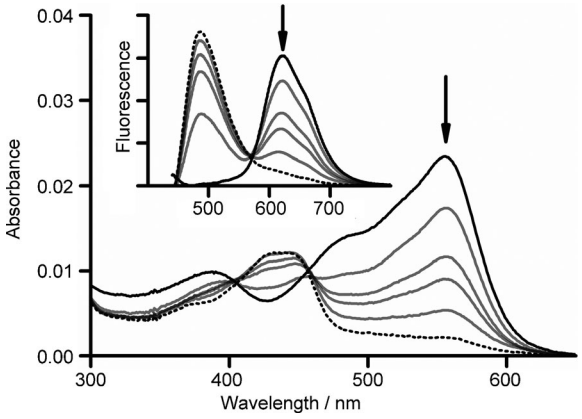

Figure 8. Absorption spectra for 1 μM **1a**/250 μM CB[7] at different pH values. Following the arrow: pH 6.9 (——), 4.0, 3.6, 3.4, 3.1, and 2.6 (••••). Inset: Fluorescence spectra for 1 μM **1a**/250 μM CB[7] at different pH values.

The protonation of **1a**@CB[7] to form **1aH**$^+$@CB[7] was confirmed in the steady-state fluorescence experiments in which the increase in the fluorescence peak at $\lambda = 488$ nm and the decrease of that at $\lambda = 621$ nm were observed with the addition of HCl (Figure 8, inset). It is likely that **1a**, which is too large to fit completely in CB[7], as indicated in Figure 1, is only partially encapsulated in the CB[7] cavity. The phenyliminium moiety of **1aH**$^+$ is a suitable binding site for CB[7] because the phenyl ring can fit into the CB[7] cavity by hydrophobic effects, and the iminium ion can coordinate to the carbonyl groups at the portal of CB[7] by ion–dipole interactions. The observation that pH changes influence the binding behavior is also consistent with this picture because the imine group is the protonation site for **1a**. The binding affinity of **1aH**$^+$ to CB[7] should be higher than that of **1a** to CB[7] ($(4.18 \pm 0.09) \times 10^4\ M^{-1}$) due to the additional driving force (i.e., ion–dipole interaction between **1aH**$^+$ and CB[7]). However, the full protonation of **1a** was achieved only in strongly acidic aqueous media (i.e., at pH ≈ 0.2), in which competition between the hydronium ion with **1aH**$^+$ for the binding sites of CB[7] was strong and the ionic strength was high.[16a] The determination of the binding constant for **1aH**$^+$@CB[7] would require the development of a sophisticated methodology, which falls outside of the scope of this paper.

Stabilization of 1a by complexation with CB[7]

Compound **1a** was photostable in CH_3CN, and no UV/Vis spectral changes were observed for solutions of **1a** in CH_3CN exposed to ambient light for days. On the contrary, rapid photobleaching of **1a** in water was observed under room fluorescent light. Specifically, exposure of 2.5 μM solutions of **1a** to room fluorescent light for 3 min led to a loss of 15% of **1a** (Figure S6 in the Supporting Information). Moreover, the extent of photobleaching was reduced by the addition of CB[7], as suggested by the decrease of the amplitude of the decay (Figure 9). These observations indicate that complexation with CB[7] in aqueous solution stabilizes **1a** kinetically and thermodynamically.

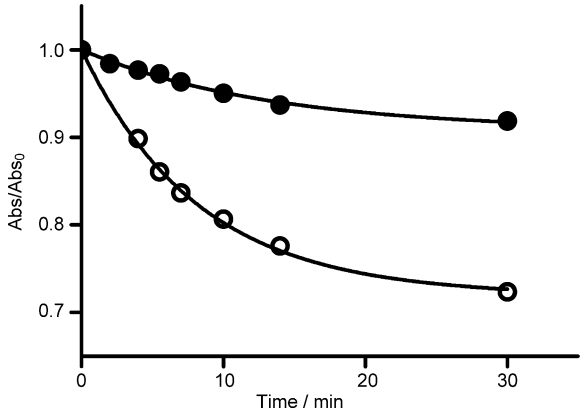

Figure 9. Temporal evolution of the absorption intensity of an aqueous solution of **1a** (2.5 μM) in the absence (○) or presence (●) of 250 μM CB[7] following irradiation at $\lambda = 430$ nm. The black curve represents the fit of data with a monoexponential decay function. The absorption intensities were recorded at $\lambda = 474$ nm for free **1a** in water or at $\lambda = 556$ nm for **1a** in the presence of CB[7] and were normalized to 100% at time 0.

Conclusion

SQ compounds have attracted increasing attention in the past decade for applications in bioimaging, photovoltaics, and numerous other technologically important areas of materials science and photochemistry, but the 1,2-isomers have only become synthetically accessible in recent years and remain relatively little explored. We have reported herein the synthesis and photophysical and electrochemical properties of the first imine derivatives of symmetric 1,2-SQs prepared from ethylbenzothiazole. 1,2-Hemiquarimines carrying one phenylimine group, either unsubstituted (**1a**) or derivatized in the *meta* position for added functionality with a bromine atom (**1b**) or a $-CO_2Me$ (**1c**) group, were synthesized in one step from the corresponding 1,2-diketones by MW irradiation and in the presence of a Lewis acid. In CH_3CN, the reported HSQiMs exhibited high molar absorption coefficients and fluorescence in the visible region. The imine group could be protonated and the resulting species showed an absorption band at lower energy and a redshifted fluorescence with a higher emission quantum yield. From the electrochemical measurements, the

redox potential of the lowest excited state was substantially higher than that of the conduction band of TiO_2; an important property for photovoltaic applications. Encapsulation in molecular hosts was successfully used to prevent aggregation, increase photostability, and enhance the photophysical properties of organic fluorophores or chromophores,[16,19] and this strategy was applied to aqueous solutions of **1a**, which were less photostable than those in CH_3CN. Encapsulation of **1a** in CB[7] led to the formation of a 1:1 complex (**1a**@CB[7]) with a binding constant of $10^4\,M^{-1}$. Complexed **1a** exhibited fluorescence enhancement and increased photostability in water. These observations make complexation with CB[7] a promising strategy for further expanding the applications of **1a**. Current work is aimed at selecting alternative Lewis acid activation to increase the 1,2-HSQiM yield and at investigating the binding of **1a**@CB[7] on nanostructured TiO_2 films for charge transfer and sensitization studies.

Experimental Section

Materials

Unless otherwise stated, all reagents and solvents were used as received from Sigma–Aldrich. *N*-Ethyl benzothiazolium iodide **1**,[9] **4**,[9] and CB[7][23, 13a] were synthesized according to published procedures. Flash chromatography was performed over SiO_2 (Macherey–Nagel 60 M, 0.04–0.063 nm, 230–400 mesh, dried at 130 °C for 60 min) or neutral alumina (Acros Organics, 50–200 mm, activity 1, dried at 130 °C for 30 min). The concentration of the CB[7] stock solutions was determined by titration with a known concentration of cobaltocenium hexafluorophosphate, according to the method developed by Yi and Kaifer.[24] Deionized water was freshly prepared by using a water purification system (Millipore synergy-UV; $\geq$18.2 MΩ cm; pH 6.9). Stock solutions of aqueous HCl (1.0 M) in deionized water, **1a** (394 μM) in CH_3CN, and CB[7] (733 μM) in deionized water were prepared and used to obtain lower concentration solutions. Solutions containing derivative **1a** were handled and stored in the dark to prevent photodegradation.

Instrumentation

^1H and ^{13}C NMR spectra were collected on 300 and 75 MHz Bruker spectrometers, respectively, at 300 K. [D_6]DMSO and all deuterated solvents were purchased from Sigma–Aldrich and used as received. IR spectra were recorded on a Thermo Scientific Nicolet 6700 FTIR spectrometer. Raman spectra were recorded with an Invia Renishaw Raman microspectrometer by using the $\lambda = 633$ nm laser line of an He–Ne laser at room temperature with a low laser power. The high-resolution mass spectra (HRMS ESI-TOF) were collected on a Mariner Perceptive Biosystem. Melting points were recorded on a Thermo Scientific Q20 DSC apparatus. 1,2-HSQiMs were prepared on a CEM Discover MW apparatus, equipped with air-cooled and power-control systems.

Photophysical measurements in organic solvents

The experiments were carried out in solutions of air-equilibrated acetonitrile at 298 K. UV/Vis absorption spectra were recorded on a PerkinElmer λ650 spectrophotometer. Fluorescence spectra were obtained with a Varian Cary Eclipse spectrofluorimeter, equipped with a Hamamatsu R928 phototube. Fluorescence quantum yields were measured by following the method of Demas and Crosby[25] (standard used: solution of perylene in ethanol, $\Phi = 0.92$.[26] Fluorescence lifetime measurements were carried out on an Edinburgh FLS920 spectrofluorimeter, equipped with a TCC900 card for data acquisition in time-correlated single-photon counting experiments and Hamamatsu H5773-04 detector in a cooled housing with an LDH-P-C-405 pulsed diode laser (0.1 ns time resolution). Global fitting of absorption and emission spectra was performed with the SPECFIT software.[27] The estimated experimental errors are 2 nm on the band maximum, 5% on the molar absorption coefficient and fluorescence lifetime, 10% on K_a, and 15% on the fluorescence quantum yield.

Photochemical experiments in organic solvents

Photochemical experiments were performed by using a medium-pressure mercury lamp equipped with an interference filter (Oriel) to select $\lambda = 436$ nm. The irradiated solution was contained in a spectrophotometric cell and stirred continuously. The intensity of the incident light was measured by the ferrioxalate actinometer.[28]

Photophysical measurements in aqueous solutions

UV/Vis absorption spectra were collected on a Varian Cary 500 UV/Vis/NIR spectrophotometer at room temperature. Steady-state fluorescence emission spectra were collected on a Horiba Fluorolog-3 instrument equipped with a xenon short-arc lamp source at room temperature. The excitation wavelength was set to $\lambda = 430$ nm with a monochromator bandwidth of 3 nm for both excitation and emission monochromators. The same fluorimeter was used to photobleach the sample when studying the photostability of **1a**. The excitation wavelength was selected with a monochromator. UV/Vis and fluorescence spectra were corrected by subtracting a baseline spectrum for a solution containing all chemicals, except **1a**. The pH values were determined by using an Accumet pH meter (AB15 plus, Fisher Scientific), which was calibrated daily by using three standard pH buffers (pH 2.00, 4.00, and 10.00). Quartz cuvettes (10×10 mm, Starna Cells, Inc.) were employed in the UV/Vis absorption and fluorescence experiments, unless stated otherwise.

Binding isotherm determination

The binding isotherm for **1a** binding to CB[7] in aqueous solutions was collected by the addition of stock solutions of CB[7] to an aqueous solution of **1a** (2.5 mL) and by measuring the UV/Vis spectra for **1a** in the presence of different concentrations of CB[7]. The dependence of the change in the signal for the absorbance at $\lambda = 556$ nm on the concentration of CB[7] was fit with a 1:1 CB[7]/**1a** binding model [Eq. (1)][29] by using the program Origin (OriginLab Inc.).

$$\Delta I = \frac{\Delta I_{max} K[CB[7]]}{1 + K[CB[7]]} \quad (1)$$

in which ΔI_{max} represents the signal changes between two conditions in which **1a** is free in water and completely bound to CB[7]; K represents the equilibrium binding constant for **1a**/CB[7] complexation.

Electrochemistry

The experiments were carried out in argon-purged CH_3CN at room temperature. In CV, the working electrode was a glassy carbon electrode (0.08 cm^2), the counter electrode was a Pt spiral, and a silver wire was employed as a quasi-reference electrode (AgQRE).

The potentials reported were referenced to SCE by measuring the AgQRE potential with respect to ferrocene ($E_{1/2}=0.39$ V vs. SCE for Fc^+/Fc). The concentration of the compounds examined was of the order of 1×10^{-3} M; 0.1 M $TEAPF_6$ was added as a supporting electrolyte. Cyclic voltammograms were obtained with scan rates in the range of 0.05–10 $V s^{-1}$. The estimated experimental error on the $E_{1/2}$ value was ±10 mV.

DFT calculations

Geometry optimization and DFT calculations were performed by using the Spartan '10 software package (Wavefunction, Inc.). DFT geometry optimization of the ground states of **4** and **1a** was performed by using the density functional B3LYP 6-31G* in vacuum.

1,2-HSQiMs 1a–c: General procedure

A solution of **4** in a suitable aniline was introduced into a MW tube, equipped with a stirring bar under a nitrogen atmosphere. $Ti(OiPr)_4$ was added to this solution and the resulting suspension was heated to 80–90 °C by MW irradiation under vigorous stirring for 2.5–8 min. The resulting suspension was treated with a saturated aqueous solution of ammonium chloride (50 mL) and extracted with CH_2Cl_2 (3×75 mL). The combined organic layers were washed with 2 M HCl (30 mL), dried over $MgSO_4$, and evaporated under reduced pressure. The residue was purified by flash column.

1,2-HSQiM 1a: 1,2-SQ **4** (130.1 mg, 0.301 mmol), aniline (2.6 mL), $Ti(OiPr)_4$ (260 μL, 0.924 mmol), 90 °C, 100 W, 5 min. Flash chromatography purification over neutral Al_2O_3 (eluent: toluene/AcOEt 9:1) gave a dark-red solid (31.6 mg, 20.5%). ^{1}H NMR (300 MHz, [D_6]DMSO, 25 °C): $\delta=7.71$ (d, $J=7.7$ Hz, 1H), 7.58 (d, $J=7.7$ Hz, 1H), 7.44–7.20 (m, 8H), 7.20–7.12 (m, 1H), 7.10–6.99 (m, 2H), 5.97 (s, 1H), 5.76 (s, 1H), 4.38–4.25 (m, 2H), 4.24–4.10 (m, 2H), 1.38–1.25 ppm (m, 6H); ^{13}C NMR (75 MHz, [D_6]DMSO, 25 °C): $\delta=183.3$, 169.5, 166.1, 159.7, 155.9, 151.6, 148.1, 141.1, 140.6, 137.4, 128.8, 128.2, 128.1, 126.9, 126.7, 126.6, 125.9, 125.3, 123.2, 122.9, 122.8, 121.9, 121.7, 119.0, 111.1, 110.2, 82.4, 81.5, 11.6, 11.4 ppm; FTIR (NaCl, thin film): $\tilde{\nu}=3058$–2852, 1719, 1653, 1586 cm^{-1}; HRMS (ESI-TOF): *m/z* calcd for $C_{30}H_{26}N_3OS_2^+$ $[M+H]^+$: 508.151; found: 508.149.

1,2-HSQiM 1b: 1,2-SQ **4** (160.4 mg, 0.371 mmol), 3-bromoaniline (3.3 mL), $Ti(OiPr)_4$ (245 μL, 0.871 mmol), 84 °C, 65 W, 8 min. Flash chromatography over SiO_2 (eluent: toluene/AcOEt 1:1, then 1:3) gave a red solid with green metallic flecks (45.9 mg, 21%). ^{1}H NMR (300 MHz, [D_6]DMSO, 25 °C): $\delta=7.73$ (d, $J=7.7$ Hz, 1H), 7.63 (d, $J=7.7$ Hz, 1H), 7.50–7.05 (m, 10H), 5.95 (s, 1H), 5.77 (s, 1H), 4.32 (q, $J=6.5$ Hz, 2H), 4.19 (q, $J=6.5$ Hz, 2H), 1.38–1.25 ppm (m, 6H); ^{13}C NMR (75 MHz, [D_6]DMSO, 25 °C): $\delta=182.6$, 170.3, 165.4, 160.8, 156.2, 152.5, 149.8, 141.0, 140.5, 130.0, 128.9, 128.2, 126.8, 126.7, 126.6, 126.0, 125.5, 125.2, 122.8, 122.3, 122.0, 121.8, 121.1, 112.7, 111.1, 110.4, 82.2, 81.6, 11.6, 11.4 ppm; FTIR (NaCl, thin film): $\tilde{\nu}=$ 3062–2871, 1720, 1651, 1582 cm^{-1}; HRMS (ESI-TOF): *m/z* calcd for $C_{30}H_{25}BrN_3OS_2^+$ $[M+H]^+$: 586.062; found: 586.074.

1,2-HSQiM 1c: 1,2-SQ **4** (112.1 mg, 0.259 mmol), ethyl 3-amminobenzoate (3.1 mL) at 45 °C, $Ti(OiPr)_4$ (245 μL, 0.871 mmol), 82 °C, 30 W, 2.5 min. Chromatography over SiO_2 (eluent: toluene/AcOEt 9:1, then 1:1 and lastly 1:3 with 5% MeOH) gave a red solid with green metallic flecks (53.1 mg, 35.4%). ^{1}H NMR (300 MHz, [D_6]DMSO, 25 °C): $\delta=7.80$–7.71 (m, 3H), 7.64–7.58 (m, 2H), 7.45–7.24 (m, 5H), 7.15 (t, $J=7.4$ Hz, 1H), 7.07 (t, $J=7.4$ Hz, 1H), 5.97 (s, 1H), 5.77 (s, 1H), 4.36–4.18 (m, 6H), 1.36–1.25 ppm (m, 9H); ^{13}C NMR (75 MHz, [D_6]DMSO, 25 °C): $\delta=182.1$, 169.9, 165.9, 160.9, 156.0, 152.9, 148.1, 140.9, 140.6, 130.0, 128.9, 128.5, 128.2, 127.1, 126.9, 126.7, 126.5, 126.0, 123.7, 123.0, 122.8, 122.3, 122.0, 121.8, 111.2, 110.5, 82.2, 60.6, 14.2, 14.1, 11.6, 11.5, 11.4 ppm; FTIR (NaCl, thin film): $\tilde{\nu}=3062$–2872, 1715, 1652, 1587 cm^{-1}; HRMS (ESI-TOF): *m/z* calcd for $C_{33}H_{30}N_3O_3S_2^+$ $[M+H]^+$: 580.172; found: 580.167.

Acknowledgements

P.C. thanks the European Commission (ERC StG*PhotoSi* 278912) for financial support. C.D.F. thanks FIS SpA for a PhD scholarship. MIUR (FIRB project *NANOSOLAR* RBAP11C58Y), the University of Padova (*Progetto Strategico HELIOS* STPD08RCX5, PRAT CPDA119117/11), and *Regione del Veneto* (SMUPR n. 4148, *Polo di ricerca nel settore fotovoltaico*) are gratefully acknowledged for financial support. E.G. is grateful to the National Science Foundation (CHE-1213669) and to the Petroleum Research Fund (PRF 4663-AC10) for research support, to Rutgers University for a Sabbatical Leave, and to the University of Padova for a Visiting Scientist Grant.

Keywords: cucurbiturils · dyes/pigments · host–guest systems · photochemistry · sensitizers · squaraines

[1] a) A. Ajayaghosh, *Acc. Chem. Res.* **2005**, *38*, 449–459; b) L. Beverina, P. Salice, *Eur. J. Org. Chem.* **2010**, 1207–1225.

[2] a) F. Silvestri, M. D. Irwin, L. Beverina, A. Facchetti, G. A. Pagani, T. J. Marks, *J. Am. Chem. Soc.* **2008**, *130*, 17640–17641; b) G. Wei, S. Wang, K. Renshaw, M. E. Thompson, S. R. Forrest, *ACS Nano* **2010**, *4*, 1927–1934.

[3] a) J.-Y. Li, C.-Y. Chen, C.-P. Lee, S.-C. Chen, T.-H. Lin, H.-H. Tsai, K.-C. Ho, C.-G. Wu, *Org. Lett.* **2010**, *12*, 5454–5457; b) H. Choi, R. Nicolaescu, S. Paek, J. Ko, P. V. Kamat, *ACS Nano* **2011**, *5*, 9238–9245; c) Y. Shi, R. B. M. Hill, J.-H. Yum, A. Dualeh, S. Barlow, M. Grätzel, S. R. Marder, M. K. Nazeeruddin, *Angew. Chem.* **2011**, *123*, 6749–6751; *Angew. Chem. Int. Ed.* **2011**, *50*, 6619–6621; d) H. Choi, P. K. Santra, P. V. Kamat, *ACS Nano* **2012**, *6*, 5718–5726; e) G. de Miguel, M. Marchena, B. Cohen, S. S. Pandey, S. Hayase, A. Douhal, *J. Phys. Chem. C* **2012**, *116*, 22157–22168; f) J. Park, C. Barolo, F. Sauvage, N. Barbero, C. Benzi, P. Quagliotto, S. Coluccia, D. Di Censo, M. Grätzel, M. K. Nazeeruddin, G. Viscardi, *Chem. Commun.* **2012**, *48*, 2782–2784.

[4] P. Salice, E. Ronchi, A. Iacchetti, M. Binda, D. Natali, W. Gomulya, M. Manca, M. A. Loi, M. Iurlo, F. Paolucci, M. Maggini, G. A. Pagani, L. Beverina, E. Menna, *J. Mater. Chem. C* **2014**, *2*, 1396–1399.

[5] a) K.-Y. Law, *J. Phys. Chem.* **1995**, *99*, 9818–9824; b) E. Terpetschnig, H. Szmacinski, A. Ozinskas, J. R. Lakowicz, *Anal. Biochem.* **1994**, *217*, 197–204.

[6] G. Wei, S. Wang, K. Sun, M. E. Thompson, S. R. Forrest, *Adv. Energy Mater.* **2011**, *1*, 184–187.

[7] a) T. Geiger, S. Kuster, J.-H. Yum, S.-J. Moon, M. K. Nazeeruddin, M. Grätzel, F. Nüesch, *Adv. Funct. Mater.* **2009**, *19*, 2720–2727; b) M. J. Paterson, L. Blancafort, S. Wilsey, M. A. Robb, *J. Phys. Chem. A* **2002**, *106*, 11431–11439.

[8] L. Beverina, M. Drees, A. Facchetti, M. Salamone, R. Ruffo, G. A. Pagani, *Eur. J. Org. Chem.* **2011**, 5555–5563.

[9] E. Ronchi, R. Ruffo, S. Rizzato, A. Albinati, L. Beverina, G. A. Pagani, *Org. Lett.* **2011**, *13*, 3166–3169.

[10] A. Aguilar-Aguilar, E. Peña-Cabrera, *Org. Lett.* **2007**, *9*, 4163–4166.

[11] L. Beverina, R. Ruffo, C. M. Mari, G. A. Pagani, M. Sassi, F. De Angelis, S. Fantacci, J.-. Yum, M. Grätzel, M. K. Nazeeruddin, *ChemSusChem* **2009**, *2*, 621–624.

[12] a) M. Freitag, E. Galoppini, *Energy Environ. Sci.* **2011**, *4*, 2482; b) C. Pagba, G. Zordan, E. Galoppini, E. L. Piatnitski, S. Hore, K. Deshayes, P. Piotrowiak, *J. Am. Chem. Soc.* **2004**, *126*, 9888–9889; c) S. A. Haque, J. S. Park, M. Srinivasarao, J. R. Durrant, *Adv. Mater.* **2004**, *16*, 1177–1181; d) H. Choi, S. O. Kang, J. Ko, G. Gao, H. S. Kang, M.-S. Kang, M. K. Nazeeruddin, M. Grätzel, *Angew. Chem.* **2009**, *121*, 6052–6055; *Angew. Chem. Int. Ed.* **2009**, *48*, 5938–5941; e) Y. Ishida, R. Kulasekharan, T. Shimada, S.

Takagi, V. Ramamurthy, *Langmuir* **2013**, *29*, 1748 – 1753; f) M. Porel, A. Klimczak, M. Freitag, E. Galoppini, V. Ramamurthy, *Langmuir* **2012**, *28*, 3355 – 3359.

[13] a) J. Kim, I.-S. Jung, S.-Y. Kim, E. Lee, J.-K. Kang, S. Sakamoto, K. Yamaguchi, K. Kim, *J. Am. Chem. Soc.* **2000**, *122*, 540 – 541; b) J. Lagona, P. Mukhopadhyay, S. Chakrabarti, L. Isaacs, *Angew. Chem.* **2005**, *117*, 4922 – 4949; *Angew. Chem. Int. Ed.* **2005**, *44*, 4844 – 4870.

[14] a) L. Isaacs, *Chem. Commun.* **2009**, 619 – 629; b) S. Liu, C. Ruspic, P. Mukhopadhyay, S. Chakrabarti, P. Y. Zavalij, L. Isaacs, *J. Am. Chem. Soc.* **2005**, *127*, 15959 – 15967; c) M. V. Rekharsky, H. Yamamura, Y. H. Ko, N. Selvapalam, K. Kim, Y. Inoue, *Chem. Commun.* **2008**, 2236 – 2238; d) M. Shaikh, J. Mohanty, P. K. Singh, W. M. Nau, H. Pal, *Photochem. Photobiol. Sci.* **2008**, *7*, 408 – 414; e) S. Moghaddam, Y. Inoue, M. K. Gilson, *J. Am. Chem. Soc.* **2009**, *131*, 4012 – 4021; f) I. W. Wyman, D. H. Macartney, *Org. Biomol. Chem.* **2008**, *6*, 1796 – 1801.

[15] a) M. R. Eftink, M. L. Andy, K. Bystrom, H. D. Perlmutter, D. S. Kristol, *J. Am. Chem. Soc.* **1989**, *111*, 6765 – 6772; b) W. C. Cromwell, K. Bystrom, M. R. Eftink, *J. Phys. Chem.* **1985**, *89*, 326 – 332; c) R. I. Gelb, L. M. Schwartz, *J. Inclusion Phenom. Mol. Recognit. Chem.* **1989**, *7*, 537 – 543.

[16] a) H. Tang, D. Fuentealba, Y. H. Ko, N. Selvapalam, K. Kim, C. Bohne, *J. Am. Chem. Soc.* **2011**, *133*, 20623 – 20633; b) R. Neugebauer, W. Knoche, *J. Chem. Soc., Perkin Trans. 2* **1998**, 529 – 534; c) C. Marquez, R. R. Hudgins, W. M. Nau, *J. Am. Chem. Soc.* **2004**, *126*, 5806 – 5816; d) R. Hoffmann, W. Knoche, C. Fenn, H.-J. Buschmann, *J. Chem. Soc., Faraday Trans.* **1994**, *90*, 1507 – 1511; e) A. E. Kaifer, W. Li, S. Silvi, V. Sindelar, *Chem. Commun.* **2012**, *48*, 6693 – 6695; f) J. Kalmár, S. B. Ellis, M. T. Ashby, R. L. Halterman, *Org Lett.* **2012**, *14*, 3248 – 3251; g) W. L. Mock, N. Y. Shih, *J. Org. Chem.* **1986**, *51*, 4440 – 4446; h) W. L. Mock, N. Y. Shih, *J. Am. Chem. Soc.* **1989**, *111*, 2697 – 2699.

[17] J. Mohanty, W. M. Nau, *Angew. Chem.* **2005**, *117*, 3816 – 3820; *Angew. Chem. Int. Ed.* **2005**, *44*, 3750 – 3754.

[18] a) S. Gadde, E. K. Batchelor, A. E. Kaifer, *Chem. Eur. J.* **2009**, *15*, 6025 – 6031; b) D. Das, O. A. Scherman, *Isr. J. Chem.* **2011**, *51*, 537 – 550.

[19] a) A. C. Bhasikuttan, J. Mohanty, W. M. Nau, H. Pal, *Angew. Chem.* **2007**, *119*, 4198 – 4200; *Angew. Chem. Int. Ed.* **2007**, *46*, 4120 – 4122; b) M. Freitag, L. Gundlach, P. Piotrowiak, E. Galoppini, *J. Am. Chem. Soc.* **2012**, *134*, 3358 – 3366.

[20] M. Freitag, E. Galoppini, *Langmuir* **2010**, *26*, 8262 – 8269.

[21] M. Tommasini, C. Castiglioni, M. Del Zoppo, G. Zerbi, *J. Mol. Struct.* **1999**, *480 – 481*, 179 – 188.

[22] a) C. Marquez, W. M. Nau, *Angew. Chem.* **2001**, *113*, 4515 – 4518; *Angew. Chem. Int. Ed.* **2001**, *40*, 4387 – 4390; b) A. L. Koner, W. M. Nau, *Supramol. Chem.* **2007**, *19*, 55 – 66.

[23] J. Zhao, H.-J. Kim, J. Oh, S.-Y. Kim, J. W. Lee, S. Sakamoto, K. Yamaguchi, K. Kim, *Angew. Chem.* **2001**, *113*, 4363 – 4365; *Angew. Chem. Int. Ed.* **2001**, *40*, 4233 – 4235.

[24] S. Yi, A. E. Kaifer, *J. Org. Chem.* **2011**, *76*, 10275 – 10278.

[25] G. A. Crosby, J. N. Demas, *J. Phys. Chem.* **1971**, *75*, 991 – 1024.

[26] M. Montalti, A. Credi, L. Prodi, M. T. Gandolfi, *Handbook of Photochemistry*, 3rd ed., CRC Taylor & Francis, Boca Raton, **2006**.

[27] SPECFIT, Spectrum Software Associates, Chapel Hill, **1996**.

[28] C. G. Hatchard, C. A. Parker, *Proc. R. Soc. London, Ser. A* **1956**, *235*, 518 – 536.

[29] a) K. A. Connors, *Binding constants: The Measurement of Molecular Complex Stability*, Wiley, New York, **1987**; b) T. C. Barros, K. Stefaniak, J. F. Holzwarth, C. Bohne, *J. Phys. Chem. A* **1998**, *102*, 5639 – 5651.

Received: January 6, 2014
Published online on April 3, 2014

